A. Kenny

A. Palazzolo

Department of Mechanical Engineering,
Texas A&M University,
College Station, TX 77843-3123

G. T. Montague

A. F. Kascak

NASA Lewis Research Center,
Cleveland, OH

Theory and Test Correlation for Laminate Stacking Factor Effect on Homopolar Bearing Stiffness

The effect of the laminate stacking factor on homopolar magnetic bearing performance is examined. Stacked laminates are used on the bearing rotor and in the stator. These laminate stacks have anisotropic permeability. Equations for the effect of the stacking factor on homopolar bearing position stiffness are derived. Numerical results are calculated and compared to measurements. These results provide an answer for the common discrepancy between test and theory for homopolar magnetic bearing position stiffnesses.
[DOI: 10.1115/1.1615258]

Introduction

Magnetic bearings often use lamination stacks in the stator poles and on the rotor. They reduce eddy current losses generated both by the rotor turning in the magnetic field and by time variation of the magnetic field. In homopolar magnetic bearings, the bias flux field travels axially through the rotor which is normal to the laminate stacks on the rotor. Figure 1 shows how the bias flux path crosses the laminated cross section of a homopolar bearing. The bias flux travels tangential to the laminates in the stator stacks, [1].

Laminate Stack Permeability

In 1980, M. L. Barton [2] published a derivation giving equations for the anisotropic relative permeability of a stack of laminates. The derivation of the relative permeability normal to the stack starts with Gauss's law, Eq. (1).

$$\nabla \cdot \mathbf{B} = 0 \tag{1}$$

This equation requires the normal flux density, B_n, at the laminate surfaces be continuous. Equation (2) then follows since the laminates are separated by a thin layer of air or adhesive.

$$B_{\text{stack}n} = \mu_o H_{\text{air}n} = \mu_{\text{lam}} \mu_o H_{\text{lam}n} \tag{2}$$

From Ampere's law an equation relating the normal magnetic field in the laminate and layer of adjoining air is given by Eq. (3).

$$l_{\text{total}} H_{\text{stack}n} = l_{\text{lam}} H_{\text{lam}n} + l_{\text{air}} H_{\text{air}n} \tag{3}$$

The definition of the stacking fraction, $f = l_{\text{lam}}/l_{\text{total}}$, combined with Eqs. (2) and (3) leads to Eq. (4). This is the dependence of the normal relative permeability of the stack on the stacking factor.

$$\mu_{\text{stack}n} = \frac{1}{\mu_o}\frac{B_{\text{stack}n}}{H_{\text{stack}n}} = \frac{\mu_{\text{lam}}}{(1-f)\mu_{\text{lam}} + f} \tag{4}$$

A similar derivation using the tangential field boundary condition leads to the relative tangential permeability of the stack given by Eq. (5).

$$\mu_{\text{stack}t} = \frac{1}{\mu_o}\frac{B_{\text{stack}t}}{H_{\text{stack}t}} = [f\mu_{\text{lam}} + (1-f)] \tag{5}$$

For a stack made out of any ferromagnetic material, the relative permeability tangential to the stack is practically given by $f\mu_{\text{lam}}$ because the stacking factor, f is just slightly less than one.

There is a dramatic difference between the relative permeability of the stack tangential and normal to the stack. Only the normal permeability is highly sensitive to the stacking factor. Figure 2 is a plot of the relative permeability of a stack versus stacking factor. Laminate stacks usually have a stacking factor less than .995 and have low values of normal permeability. These are used in the three-dimensional finite element analysis of electric machinery. For example, Timothy and Preston [3] report a using normal stack relative permeability of 20 in the finite element analysis of a large turbine generator.

Table 1 shows numerical values for the permeability normal to two stacks made from two different materials. Metal A has a value for the relative permeability μ_{lam} of 500, while metal B has a value of 5000. The effect of stacking is to make the normal permeability for both laminated stacks very much lower and almost equal. For a stacking factor of 0.99 the normal permeabilities of the two stacks differ by only 15% even though the permeabilities of the laminate metals differ by a factor of ten.

The stacking factor is affected by pressure on the laminates, laminate thickness, and the adhesive bonding technique used, [4]. Some laminate alloys require high temperature heat treatments, [5], which can affect the surface roughness and oxide thickness.

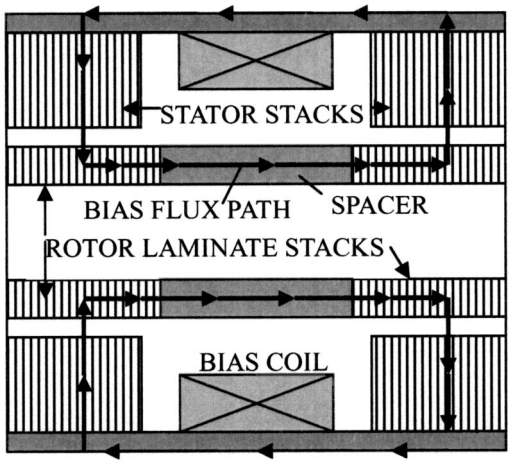

Fig. 1 Laminated bias flux path in a homopolar magnetic bearing

Contributed by the International Gas Turbine Institute (IGTI) of THE AMERICAN SOCIETY OF MECHANICAL ENGINEERS for publication in the ASME JOURNAL OF ENGINEERING FOR GAS TURBINES AND POWER. Paper presented at the International Gas Turbine and Aeroengine Congress and Exhibition, New Orleans, LA, June 4–7, 2001; Paper 2001-GT-0294. Manuscript received by IGTI, December 2000, final revision, March 2001. Associate Editor: R. Natole.

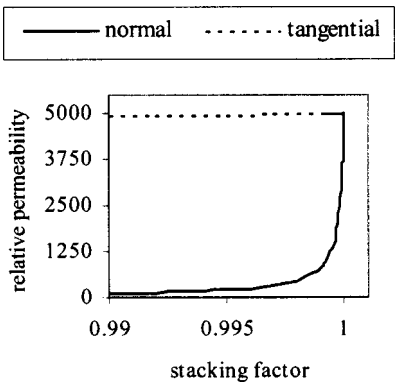

Fig. 2 Relative permeability of laminate stack

The stacking factor can be measured from the stack weight, volume, and laminate material density using Eq. (6).

$$f = \frac{\text{mass}_{\text{stack}} - \rho_a \text{vol}_{\text{stack}}}{(\rho_{\text{lam}} - \rho_a)\text{vol}_{\text{stack}}} \tag{6}$$

For cold rolled metal the surface roughness varies between 1.25 and 4.9 microns (32 and 125 micro inches), [6,7]. As shown in Fig. 3, stacking factors between .997 and .989 would result from stacked layers of .15 mm (.006 in.) cold rolled metal laminates assuming the rough regions on both sides of the laminates are air.

We made measurements on two stacks of rotor laminates made from 17.8 mm (.7 in.) and 8.8 mm (.35 in.) thick stacks of.15 mm (.006 in.) thick adhesive bonded laminates with a diameter of 44.5 mm (1.75 in.). The measurements included the stack dimensions and weight. Using the known density of the metal, the stacking factors were determined to be .981 and .987.

The stacking factor of tape wound cores tends to be lower than that of flat stacks of laminates. Table 2, [8], shows stacking factors for tape wound cores reported by one manufacturer. It indicates

Table 1 Numerical values of relative permeability of laminate stack

Stacking Factor	Metal A $\mu_{\text{stack}n}$	Metal B $\mu_{\text{stack}n}$
1.0	500	5000
.995	143	192
.99	83	98
.95	19	20
.92	12.2	12.5
.90	9.8	9.98
.85	6.6	6.7
.70	3.3	3.3
.50	2.0	2.0

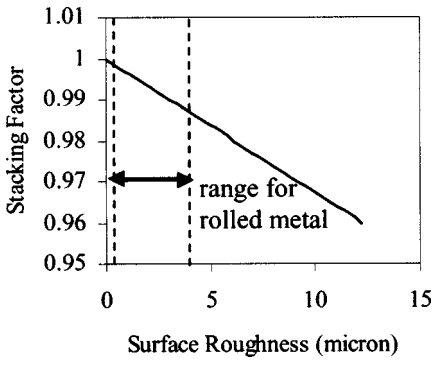

Fig. 3 Simple theoretical relation between .15-mm thick plate surface roughness and stacking factor

Table 2 Stacking factor of tape wound cores

Tape Thickness micron (in.)	Stacking Factor
205 (.012)	.95
153 (.006)	.90
102 (.004)	.90
50.8 (.002)	.85

the average separation distance between tape wound laminates is 12 to 20 microns (.0003 to .0005 in.). The stacking factor of a core wound from 80 micron (.002 in.) thick metal tape, could be as low as 0.75.

Derivation of Position Stiffness Equations Including Stacking Factor

The homopolar bearing bias flux path circuit model is illustrated in Fig. 4. The bias flux flows normal to the rotor stack laminations which have the reluctances denoted by R_{rnp_j} and R_{rns}. These reluctances are relatively high since the laminates are normal to the flux path. The bias flux travels across a variable number of rotor laminates, depending on which laminate in the stator stack it originated. Therefor there is a specific rotor reluctance, R_{rnp_j}, Eq. (7), for each laminate, j, in the stator stack.

$$R_{rnp_j} = \frac{\frac{j}{k} l_{rnp}}{\mu_{\text{stack}n} \mu_o A_{\text{lam}}} \tag{7}$$

In Fig. 4, there is a reluctance denoted by R_{rns}, for the spacer that separates the laminated rotor sections under the left and right side poles. Because the bias flux is not time varying, sometimes the spacer is not laminated. The spacer may be a laminated stack if there is a need to minimize the eddy current power loss in the bearing. The laminates reduce the eddy currents generated because the spacer is a rotating conductor in the bias flux path. Equations (8) and (9) give the reluctance for the unlaminated and laminated spacer. The cross-section area of the back iron is often designed to equal that of the rotor spacer so that they will both magnetically saturate at once. This is the reason for the same cross-section areas, A_{lam}, in both Eqs. (8) and (9).

$$R_{rs} = \frac{l_s}{\mu_{\text{lam}} \mu_o A_{\text{lam}}} \tag{8}$$

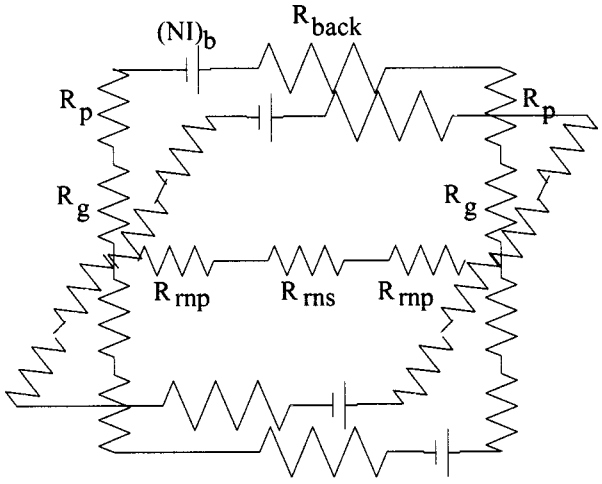

Fig. 4 Homopolar bearing bias path circuit model

$$R_{rns}=\frac{l_s}{\mu_{\text{stack}n}\mu_o A_{\text{lam}}} \tag{9}$$

The flux path width is wider in the gap since it includes the whole cross section of the laminate and the stacking factor layer. The gap cross section is therefore larger than the pole laminate by the factor $1/f$ as shown in Eqs. (10) and (11).

$$R_g=\frac{l_g}{\mu_o A_{\text{lam}}/f} \tag{10}$$

$$R_p=\frac{l_p}{\mu_{\text{lam}}\mu_o A_{\text{lam}}} \tag{11}$$

The bearing position stiffness is the ratio of the change in force on the rotor to the change in radial displacement of the shaft. Movement of the shaft alters the gap reluctance which in turn alters the bias flux and the force. The bias flux through each laminate in the pole stack is calculated via Eq. (12). For very small movements of the rotor the gap bias flux varies according to Eq. (13)–(14).

$$\Phi_{b_j}=\frac{(NI)_b}{2R_p+2R_g+R_{rns}+R_{\text{back}}+2R_{rnp_j}} \tag{12}$$

$$\Phi_{(bg+)_j}=\Phi_{b_j}\frac{l_g}{l_g+\Delta x} \tag{13}$$

$$\Phi_{(bg-)_j}=\Phi_{b_j}\frac{l_g}{l_g-\Delta x} \tag{14}$$

The magnetic force on the rotor is due to the flux density under each laminate, and the total force on the rotor is the sum of the forces from all the laminates as given by Eq. (15). The factor of two comes from the force under the two planes of the two laminated stators in this homopolar bearing. Thus the position stiffness is calculated from the limit of Eq. (16). As shown by Eq. (17), it is proportional to the square of the bias flux which is reduced by the stacking effect.

$$F_{b\text{rotor}}=2\sum_{j=1}^{k}\left(\frac{f^2\eta^2\Phi_{b+_j}^2}{2\mu_o A_{\text{lam}}}-\frac{f^2\eta^2\Phi_{b-_j}^2}{2\mu_o A_{\text{lam}}}\right) \tag{15}$$

$$K_p=\Delta x \xrightarrow{\lim} 0\ \frac{F_{b\text{rotor}}}{\Delta x} \tag{16}$$

$$Kp=\frac{4\eta^2 f^2}{l_g\mu_o A_{\text{lam}}}\sum_{j=1}^{k}\Phi_{b_j}^2 \tag{17}$$

Combining Eqs. (7)–(12) and Eq. (17) results in Eq. (18) which is the position stiffness including the effect of the stacking factor. The terms in the denominator have the greatest effect on the position stiffness. As the stacking factor decreases, the effective length of the laminated rotor spacer, l_s, and the rotor stack under the poles, l_{rnp}, increases. The squared f term in the numerator also contributes to the position stiffness decrease.

$$K_p=\frac{4(NI)_b^2 f^2\eta^2\mu_{\text{lam}}^2\mu_o A_{\text{lam}}}{l_g}\sum_{j=1}^{k}\left[\frac{1}{2\cdot l_p+l_{\text{back}}+2\cdot l_g f\mu_{\text{lam}}+\left(l_s+\frac{2j}{k}l_{rnp}\right)((1-f)\mu_{\text{lam}}+f)}\right]^2 \tag{18}$$

The bearing current stiffness is also dependent on the stacking factor. As Eq. (19) shows, it is directly proportional to the bias flux. It is reduced less by stacking than the position stiffness, since the control flux path is only tangent to the laminates.

$$K_i=\frac{8f^2\eta^2}{\mu_o A_{\text{lam}}}\frac{\partial(\phi_c)}{\partial(i)}\frac{1}{k}\sum_{j=1}^{k}\Phi_{bg_j} \tag{19}$$

The achievable bearing stiffness is affected by stacking by both the position stiffness and the current stiffness as shown by Eq. (20).

$$K_a=K_i K_{pa} K_c-K_p \tag{20}$$

Measurements and Results

Measurements of the position stiffness were made on a homopolar bearing designed for a low drag torque application. The rotor on this bearing was entirely laminated. There was no unlaminated spacer between rotor stacks under the fore and aft poles. A photograph of this bearing is shown in Fig. 5.

The measured position stiffness of this bearing was compared to the position stiffness predicted by Eq. (18). A three-dimensional magnetostatic model of the bearing was also used to predict the stiffnesses. The anisotropic relative permeability of the laminated rotor and stator was used in the FEA model rotor and stator stacks shown in Fig. 6. The relative permeabilty normal to the laminate stacks was calculated using Eq. (4), and the tangential relative permeability was calculated using Eq. (5).

The position stiffnesses that were measured and predicted are shown in Table 3. The one-dimensional circuit prediction calculated by Eq. (18) was very close to the measured value when a reasonable value for the stacking factor was used. The difference between the measured value and the one-dimensional circuit prediction was only 6.8% based on a stacking factor of .992. The

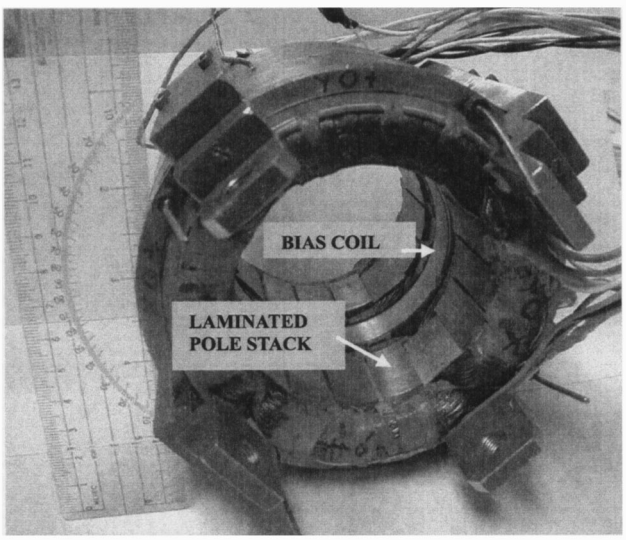

Fig. 5 Homopolar bearing for position stiffness measurements

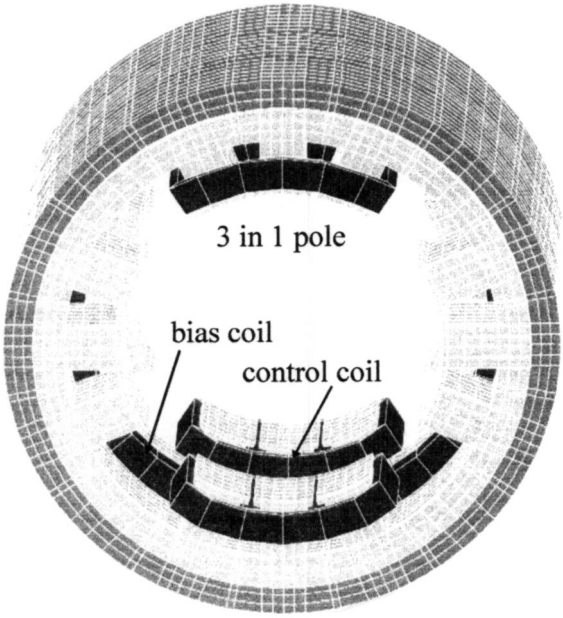

Fig. 6 Finite element model of bearing

FEA model showed similar accuracy. The difference between the FEA prediction and the measured value was only 3.3% based on a stacking factor of .993. To see the importance of including the effect of lamination, the stiffness predicted by Eq. (18) with an unlaminated rotor which would have a stacking fraction of 1.00 is included. In this case the difference between the measured value and the prediction is 153%. In other words a prediction that does not include that stacking factor cannot be expected to be close to the true value of stiffness.

Conclusions

The position stiffness in homopolar bearings is affected by the bias flux density. Since part of the bias flux path passes through the rotor normal the rotor laminate stacks, the bias flux is reduced by the low anisotropic permeability of the stack normal the laminates. The relative permeability normal to the laminate stack can be calculated using the laminate stacking factor. Then the normal relative permeability can be included in magnetic circuits and finite element models to better predict the homopolar bearing position stiffness.

Table 3 Comparison of position stiffnesses

	Position Stiffness	Percent Difference
Measured value	−1.49 MN/m −8500 LB/in	–
One-dimensional circuit Eq. (25) with $f=1.00$	−3.76 MN/m −21500 LB/in	153
One-dimensional circuit Eq. (25) with $f=.992$	−1.59 MN/m −9076 LB/in	6.8
Three-dimensional FEA model with $f=.993$	−1.44 MN/m −8218 LB/in	−3.3

Acknowledgments

The authors gratefully acknowledge the funding for this project from the Machinery Dynamics Branch and from Ray Beach each of the Space Power Systems Division at NASA Glenn Research Center. The authors also thank Mr. John Poles of NASA GRC for his excellent support in Power Electronics for the testing. The authors also gratefully acknowledge funding for this project from Tom Calvert, Lyn Peterson, and Glenn Bell of the U.S. Naval Surface Warfare Center. The authors thank Dr. David Carpenter of Vector Fields, Inc., for his expert assistance with the FEA modeling.

Nomenclature

A_{lam} = area of pole laminate flux cross section
B_g = flux density through air gap
$B_{\text{stack}n}$ = flux density normal to stack laminates
$B_{\text{stack}t}$ = flux density tangential to stack laminates
f = stacking factor
F_b = force on one pole due to bias flux
F_{bg+} = bias flux force on pole with incrementally larger gap
F_{bg-} = bias flux force on pole with incrementally smaller gap
$H_{\text{air}n}$ = magnetic field in air normal to laminate
$H_{\text{lam}n}$ = field in laminate normal to laminate
$H_{\text{stack}n}$ = field normal to stack of laminates
$H_{\text{stack}t}$ = field tangential to stack of laminates
H_t = tangential field
i = control current
j = jth laminate in stack
k = number of laminates in stack
K_a = achievable bearing stiffness
K_c = controller feedback gain
K_i = current stiffness
K_p = position stiffness of bearing
K_{pa} = power amplifier gain
l_{air} = separation distance between laminates
l_g = length of air gap
l_{lam} = laminate thickness
l_p = length of laminated pole
l_{rnp} = length of normal flux path in rotor laminates under pole
l_s = length of rotor spacer
l_{total} = total length of flux path
$\text{mass}_{\text{stack}}$ = mass of all metal and adhesive in stack
η = gap flux density fringe factor
$(NI)_b$ = bias coil current and bias coil turns
$\Phi_{(bg+)_j}$ = bias flux in larger gap under jth laminate
$\Phi_{(bg-)j}$ = bias flux in smaller gap under jth laminate
ϕ_c = control flux in gap
R_{back} = reluctance of solid back iron
R_{b_j} = reluctance of bias flux path through jth laminate
R_g = reluctance of air gap
R_p = reluctance of one laminate in pole
R_{rnp_j} = reluctance of rotor from pole laminate j to stack edge
R_{rns} = reluctance of laminated spacer on rotor
ρ_a = density of interlaminate air or adhesive
ρ_{lam} = density of ferromagnetic laminate
μ_o = permeability of air
μ_{lam} = relative permeability of ferromagnetic laminate
$\mu_{\text{stack}n}$ = relative permeability of stack normal to laminate
$\mu_{\text{stack}t}$ = relative permeability of stack tangential to laminate
$\text{vol}_{\text{stack}}$ = volume of laminate stack
Δx = incremental movement of shaft to open or close gap

References

[1] Fukata, S., Yutani, K., and Kouya, Y., 1998, ''Characteristics of Magnetic Bearings Biased With Permanent Magnets in the Stator,'' JSME Int. J., Ser. C, **41**(2), pp. 206–213.

[2] Barton, M. L., 1980, ''Loss Calculation in Laminated Steel Utilizing Anisotropic Magnetic Permability,'' IEEE Trans. Power Appar. Syst., **PAS-99**(3), pp. 1280–1287.

[3] Timothy, M. A., and Preston, T. W., 1995, ''Finite Element Modeling of Laminated Structures in Electrical Machines,'' *Proceedings IEE, 7th International Conference on Electrical Machines and Drives*, Institution of Electrical Engineers, London, pp. 121–125.

[4] De Weese, R. T., 1996, ''A Comparison of Eddy Current Effects in a Single Sided Magnetic Thrust Bearing,'' thesis, Texas A&M University, College Station, TX.

[5] Kondoleon, A. S., 2000, ''Soft Magnetic Alloys for High Temperature Radial Magnetic Bearings,'' *Proceedings 7th International Symposium on Magnetic Bearings*, ETH-Zurich (Swiss Federal Institute of Technology), Zurich, Switzerland, pp. 111–116.

[6] Beausmeister, T., et al., ed., 1978, *Mark's Standard Handbook for Mechanical Engineers*, 8th Ed., McGraw-Hill, New York.

[7] Rastogi, P. K., 1988, ''Lamination Steel Technology for Appliance Industry,'' IEEE Trans. Ind. Appl., **24**(6), pp. 982–986.

[8] Magnetic Metals Inc., 2000, *Tape Wound Core Design Manual*, Westiminister, CA.